

Influence of Cladding and Shape of Defect on the Critical Crack Size at a PWR Vessel Beltline During an Intermediate LOCA

J. Vagner, D. Guichard

Framatome, Division des Fabrications, B.P. 13, F-71380 Saint-Marcel, France

ABSTRACT

The critical sizes for defects located at the inner surface of the PWR reactor vessel beltline are determined by LEFM with plasticity correction, during an intermediate LOCA.

The influence of different parameters on critical size is examined : defect shape and position, final RTNDT, residual stresses.

1 - FOREWORD

An evaluation of the fracture resistance of the PWR 900 MWe vessels was undertaken further to a contract between EDF and FRAMATOME (ref. 1). The study of the risk of fast fracture in a PWR vessel shell poses the problem of the defect localization and shape.

We study here the effect of the shape of defects located at the inner surface of the vessel belt line. Due to the presence of cladding, we can assume the various following shapes :

- axisymmetrical cracks emerging through cladding,
- longitudinal strip cracks emerging through cladding,
- semi-elliptical cracks emerging through cladding,
- underclad strip-cracks (not emerging),
- underclad elliptical cracks (not emerging).

The calculations are performed for various RTNDT conditions and several residual stresses assumptions.

The transient retained for the analysis is an intermediate LOCA.

The study is carried out using linear elastic fracture mechanics.

2 - STUDY OF EMERGING DEFECTS

2.1 Determination of the stress intensity factor

This determination is based on the use of influence functions (ref. 2 and 3).

Due to the discontinuous stress at the clad to base metal interface, we have resolved the stress into the superposition of a through-structure continuous function and a constant value function through the clad thickness.

Influence functions relevant to this stress distribution were determined in order to comply with the discontinuity.

2.2 Determination of the residual stresses in cladding

The residual manufacturing stresses are added to the thermal and pressure stresses due to the transients.

For determining these residual stresses, we have performed an elastoplastic numerical simulation of the cooling process after stress relief heat treatment, followed by the hydrotest, by assuming a stress level equal to zero at 600°C.

The variation of longitudinal and circumferential stresses in cladding is shown fig. 1. The stress level after hydrotest is then $\sigma_c = 156$ MPa and $\sigma_l = 199$ MPa.

2.3 Criterion of instability

For the longitudinal strip-defect and the axisymmetrical defect, the criterion of instability retained is :

$$K_{cp} = K_L$$

where :

K_{cp} : stress intensity factor after plasticity correction at the crack tip.

$K_L = K_{IC}$ of the base metal for a defect size greater than or equal to the clad thickness. The K_{IC} value is that of the ASME section XI reaching its maximum at 195 MPa \sqrt{m} .

$K_L = K_{JC}$, limit cladding toughness, for a defect size lower than the clad thickness : $K_{JC} = (EJ_c / 1 - \nu^2)^{1/2}$.

The clad limit K_{JC} at the end of life not being precisely known, we have retained the value of 150 MPa \sqrt{m} as a safe lower bound of the initiation toughness accounting for some stable tearing crack growth.

A value of 200 MPa \sqrt{m} is retained for the parametric analysis in order to obtain a more representative value.

For the semi-elliptical defect, we retain three criteria of instability :

- at the bottom point : $K_{cp} = K_L$ at the smallest axis of the semi-elliptical crack (K_L defined as above).
- at the edge point : $K_{cp} = K_{JC}$ (cladding toughness) at the greatest axis of the semi-elliptical crack.
- probabilistic criterion (ref. 4) $\frac{1}{LR} \int \left(\frac{K_I}{K_{IC}} \right)^4 dL < 1$ with $LR = 100$ mm

The integration is carried on along the part of the crack front in the base metal. This criterion states that the fracture probability in the analyzed crack structure is lower or equal to the probability of getting a toughness value lower than the reference curve limit $K_{IC} = f(RTNDT)$, when tests are made with specimens of width $B = L_R$.

2.4 Boundary conditions

- The shell under study is 207.5 mm thick, including a clad thickness of 7.5 mm.
- The transient studied is a small primary break whose temperature, pressure and heat transfer coefficient variations are shown fig. 2.
- The base metal RTNDT at the cladding interface is 85 °C. It decreases through the wall depth down to 31,5 °C at the outside surface.

For the semi-elliptical crack, the ratio of length over depth is chosen equal to six.

2.5 Results

The temperature and longitudinal stress variations through the wall are shown fig. 3 and 4.

The variations of K_I/K_{IC} at the crack bottom for the longitudinal strip defects and semi-elliptical defects are depicted fig. 5 as a function of time for a depth of 20 mm.

The fig. 6 shows the variation of K_I/K_{IC} along the crack front in the base metal for a semi-elliptical defect of 20 mm and a time of 3900 s.

The values of the critical crack depth for each of the above criteria are given in the line A of table 1.

We observe that :

- the emerging axisymmetrical and longitudinal strip cracks are stable when the bottom points are in the cladding, but become unstable as soon as it reaches the base metal,

- the semi-elliptical circumferential crack presents the same behaviour at the bottom point, with $K_{cp} > K_{IC}$, as soon as it reaches the interface, but the semi-elliptical longitudinal crack gives a critical crack size of 134 mm for the bottom point criterion. These differences in behaviour come from the larger value of longitudinal residual stresses acting on the circumferential crack,

- the probabilistic criterion gives similar critical sizes for the circumferential and longitudinal semi-elliptical cracks, 19.8 and 18.8 mm despite significant differences in the K_I/K_{IC} distributions, we consider this criterion as the most relevant one,

- even with the low toughness $K_{JC} = 150 \text{ MPa } \sqrt{\text{m}}$, the cracking resistance of the cladding does not constitute the weakest point.

2.6 Parametrical analysis

On the basis of the case defined in para. 2.4, we perform a series of parametric studies whose changes, compared to the base case, are the following :

case B : RTNDT = 100°C

case C : RTNDT = 64°C

case D : residual stresses in cladding : $\sigma_L = 250 \text{ MPa}$ and $\sigma_C = 200 \text{ MPa}$

case E : residual stresses 150 MPa and 120 MPa

case F : zero residual stresses

case G : no clad for K calculation

case H : K_L of cladding = 200 MPa $\sqrt{\text{m}}$

This parametric study is made easier by the performance of all calculations (temperature, stress, stress intensity factor, determination of the limit defect) using the CALORI software.

The table 1 shows a significant effect of all parameters. Particularly, the case G shows that the old practice ignoring the clad presence, leads to optimistic unreliable critical crack sizes.

This conclusion has already been reached in ref. 6 on an infinite longitudinal defect configuration.

3 - STUDY OF UNDERCLAD DEFECTS

The defects studied are either very long strip defects, or ellipses tangent to cladding, the length of the elliptical defect is considered equal to 60 mm.

3.1 Determination of the stress intensity factor

We assume the following :

$$K_I = K_{IB} \times F_B \times F_E$$

where : K_{IB} = stress intensity factor for a strip crack in infinite medium under the stress distribution.

F_B = factor due to the edge effect.

F_E = factor due to the elliptical shape ($F_E = 1$ for the strip or axis-symmetrical defects).

These factors are available in various documents.

The problem of near-edge defects is that of plasticity corrections to be applied to the elastic calculation.

In case of mechanical loading, it was demonstrated that a single correction of the IRWIN type was not sufficient to give a K_{cp} value near the value $K_J = [EJ(1-\nu^2)]^{1/2}$ obtained by an elastoplastic calculation, as soon as the plastic wing at the crack tip reaches a notable proportion of the ligament (ref. 7).

For K_{cp} calculation, we have retained 3 hypotheses :

$$K_{cp} = \alpha K_I \sqrt{\frac{2a + rc + rb}{2a}}$$

with rc : plasticity correction - clad side and rb : plasticity correction - base metal side.

- $\alpha = 1$ the edge effect on the plasticity correction is then ignored.
- $\alpha = f$ (rc , ligament value) : this correction proposed by appendice ZG of RCCM-B (ref. 5) is extrapolated beyond its limit of validity, but is limited to the value of 1.6. The limitation $\alpha < 1.6$ has been observed in an elastoplastic study carried out on a near-edge defect configuration.
- for the calculation of K_{cp} in the base metal, the two first assumptions were supplemented by a strip yield model analysis, which uses an emerging semi-elliptical crack, closed up at the clad level by a closing pressure of 350 MPa (representative value of the plastic flow stress of cladding).

3.2 Criteria of instability

A) small axis, clad side (point A), the limit dimension is obtained when $K_{cp} = K_{JC}$ (see para. 2.3).

B) small axis, opposite side (point B) $K_{cp} = K_{IC}$.

C) on the larger axis of the ellipse (point C), we have compared K_{cp} to the K_{IC} value at the clad to base metal interface so as to be pessimistic.

3.3 Results

They are shown in the Table 2. The boundary conditions in each case are the same as those of para. 2.4. The four cases A, B, C, H of the parametric analysis of para. 2.6 are considered.

The indices a, b, c enable to identify the assumption for the plasticity correction, as defined in para. 3.1.

The symbol ∞ (tables 1 and 2) means that for the case considered, the stability criterion is met with the deepest cracks analysed.

We can observe :

- that, on the clad side, the most sensitive parameters are the defect shape, the plasticity correction and the cladding toughness,
- that, on the base metal side, the RTNDT value has a significant effect on the limit size value.

4 - GENERAL CONCLUSION

The results point out the large effect of several of the factors in the parametric analysis. In particular, they emphasize the following :

- the analysis without taking into account the presence of cladding in the case of emerging defects is not mechanically relevant,
- the configuration of non-emerging underclad cracks, which is more in relation with possible manufacturing defects, leads to critical crack sizes much larger than for the configuration of cracks emerging through cladding,
- the elliptical underclad cracks are wholly stable for the base metal criterion with RTNDT equal or lower than 85°C, and these critical crack sizes then depend on the cladding toughness,
- the analysis presented here, based on linear elastic fracture mechanics, does ignore the attenuation that plastic strains may impose to the residual and thermal stresses in the cladding. This attenuation could significantly enlarge the critical crack size for the cracks emerging through cladding for the most severe case of the parametric analysis.

5 - ACKNOWLEDGEMENT

The authors thank Mr BUCHALET from FRAMATOME and Mr HEDIN and Mr NOEL from Electricité de France for their cooperation and support for this study.

6 - REFERENCES

- 1 - C. BUCHALET, P. HAUSSAIRE, B. HOUSSIN, J. VAGNER - Assessment of margins with respect to pressurized thermal shock for the 3 loop plants of french program. 3rd international SMIRT post seminar RP 6 - Monterey - California 29-30 Août 83
- 2 - R. LABBENS, A. PELLISSIER-TANON, J. HELIOT - ASTM STP 590, 1976, p. 370-384.
- 3 - J. HELIOT, R. LABBENS, A. PELLISSIER-TANON - ASTM STP 677, 1980, p. 341-364.
- 4 - A. PELLISSIER-TANON - Advances in fracture research, ICF6, 1984, vol. 1 p. 697-706.
- 5 - Design and construction rules for mechanical components of PWR nuclear islands - RCCM - AFCEN France.
- 6 - R. AHLSTRAND and all - SMIRT 6, 1981, G1/4.
- 7 - A. PELLISSIER-TANON, J.C. DEVAUX, F. ROBISSON - SMIRT 6, 1981, G6/3.

TABLE 1 - CRITICAL CRACK SIZES FOR EMERGING CRACKS (mm)

Case	Factors of parametric analysis	LONGITUDINAL CRACK				CIRCUMFERENTIAL CRACK			
		STRIP	SEMI-ELLIPTICAL			AXISYMMETRIC	SEMI-ELLIPTICAL		
		bottom	bottom (a)	edge (b)	probabilistic (c)	bottom	bottom (a)	edge (b)	probabilistic (c)
A	RTNDT = 85°C	7.5	134	86	18.8	7.5	7.5	85	19.8
B	RTNDT = 100°C	7.5	7.5	86	13.5	7.5	7.5	85	14.1
C	RTNDT = 64°C	37	134	86	50.4	7.5	7.5	85	72.2
D	larger σ_r	7.5	7.5	78	16.2	7.5	7.5	75	16.6
E	lower σ_r	9.3	134	92.5	22.3	7.5	7.5	95	27.5
F	$\sigma_r = 0$	28.4	136	111	39.5	134	174	119	67.7
G	no cladding	45.2	123	44*	53.8	134	174	53*	84.6
H	KJC = 200MPa \sqrt{m}	7.5	134	102	18.8	7.5	7.5	102	19.8

* base material toughness

TABLE 2 - CRITICAL CRACK SIZES FOR UNDERCLAD CRACKS (mm)

Factors of analysis		LONGITUDINAL CRACK						CIRCUMFERENTIAL CRACK					
Case RTNDT (°C)	Plasticity correction	STRIP			ELLIPTIC			STRIP			ELLIPTIC		
		A	B		A	B	C	A	B		A	B	C
		cladding	base M.		cladding	base M.	Base M.	cladding	base M.		cladding	Base M.	Base M.
A - 85	b	32.8	124		74.4	"	"	36.3	"	"	"	"	"
A - 85	c	63.1	79		"	"	"	68.5	"	"	"	"	"
B - 100	a	32.8	22.8		74.4	"	45.9	36.3	"	"	"	"	"
B - 100	b	32.8	24.6		"	"	"	"	"	"	"	"	"
B - 100	c	32.8	124		74.4	"	"	36.3	"	"	"	"	"
C - 64	b	49.3	124		"	"	"	54.4	"	"	"	"	"
H - 85	b	49.3	124		"	"	"	"	"	"	"	"	"

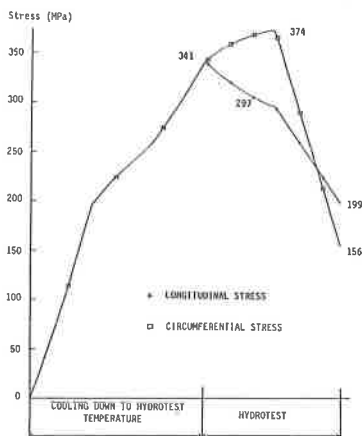


FIG. 1 - EVOLUTION OF LONGITUDINAL AND CIRCUMFERENTIAL STRESSES IN CLADDING AFTER RELIEVING HEAT TREATMENT AND DURING HYDROTEST

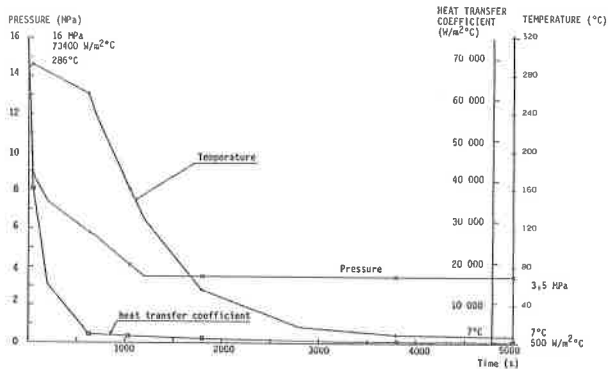


FIG. 2 - DEFINITION OF INTERMEDIATE LOCA

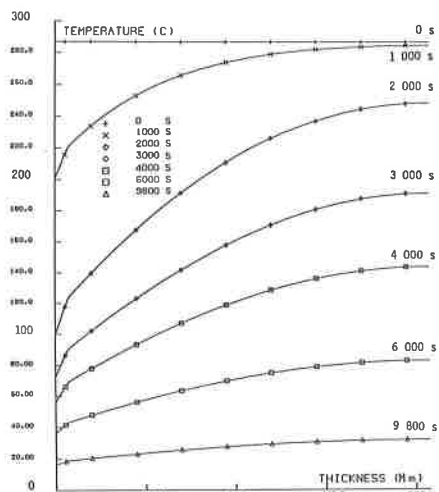


FIG. 3 - EVOLUTION OF TEMPERATURE DISTRIBUTION
AS A FUNCTION OF TIME

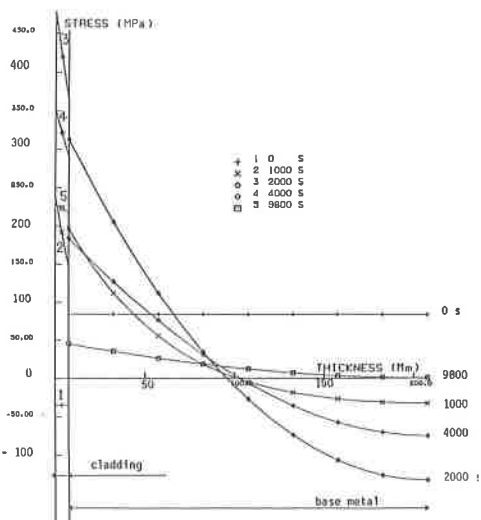


FIG. 4 - EVOLUTION OF LONGITUDINAL STRESS DISTRIBUTION
AS A FUNCTION OF TIME

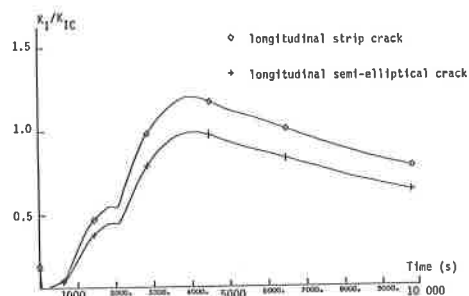


FIG. 5 - EVOLUTION OF RATIO K_1/K_{IC} AS A FUNCTION OF TIME
FOR A DEPTH OF 20 mm

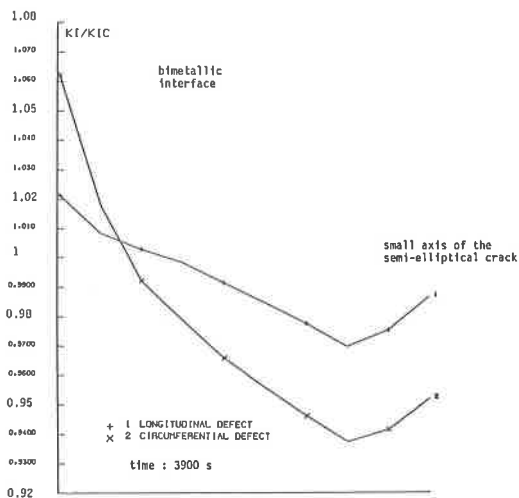


FIG. 6 - EVOLUTION OF RATIO K_1/K_{IC} ALONG THE FRONT OF THE
SEMI-ELLIPTICAL CRACK IN BASE METAL